nature

https://doi.org/10.1038/s41586-020-1996-3

Supplementary information

Loss of p53 drives neuron reprogramming in head and neck cancer

In the format provided by the authors and unedited

Moran Amit✉, Hideaki Takahashi, Mihnea Paul Dragomir, Antje Lindemann, Frederico O. Gleber-Netto, Curtis R. Pickering, Simone Anfossi, Abdullah A. Osman, Yu Cai, Rong Wang, Erik Knutsen, Masayoshi Shimizu, Cristina Ivan, Xiayu Rao, Jing Wang, Deborah A. Silverman, Samantha Tam, Mei Zhao, Carlos Caulin, Assaf Zinger, Ennio Tasciotti, Patrick M. Dougherty, Adel El-Naggar, George A. Calin✉ & Jeffrey N. Myers✉

Supplementary Figure 1. Uncropped scans with size marker indications

Extended Data Fig. 1h

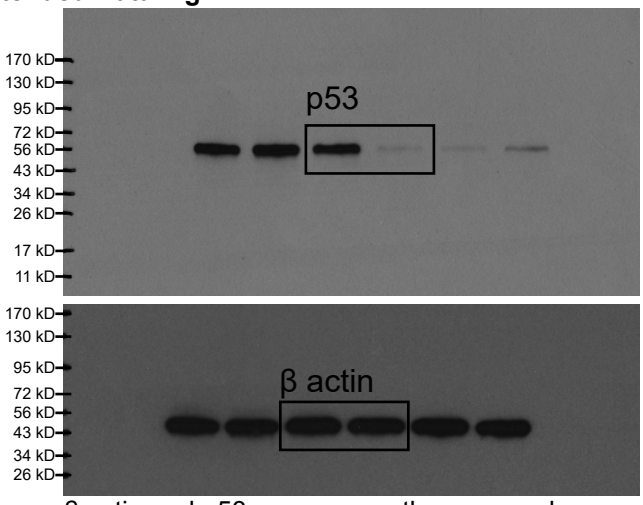

β actin and p53 were run on the same gel

Extended Data Fig. 2e

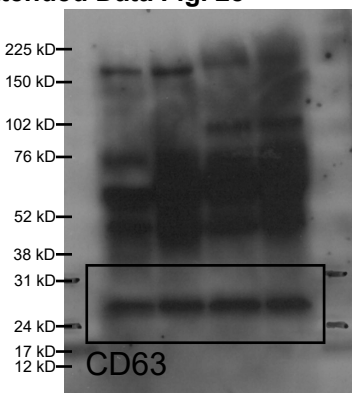

Extended Data Fig. 2f

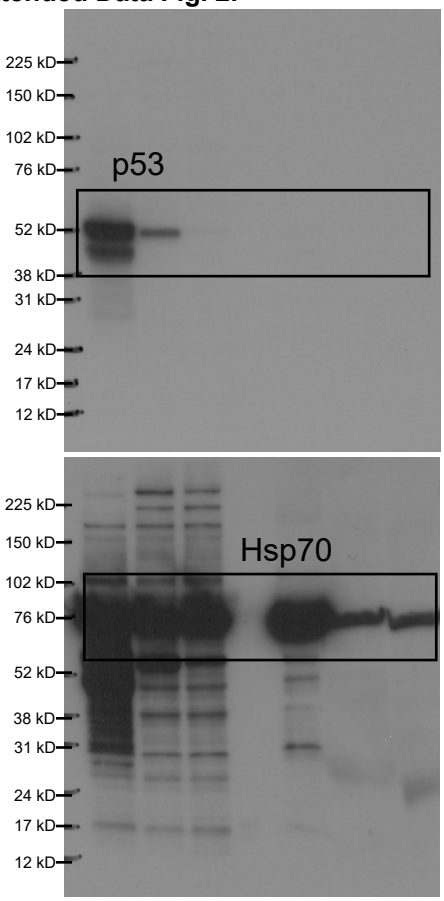

Hsp70 and p53 were run on the same gel

Extended Data Fig. 2h

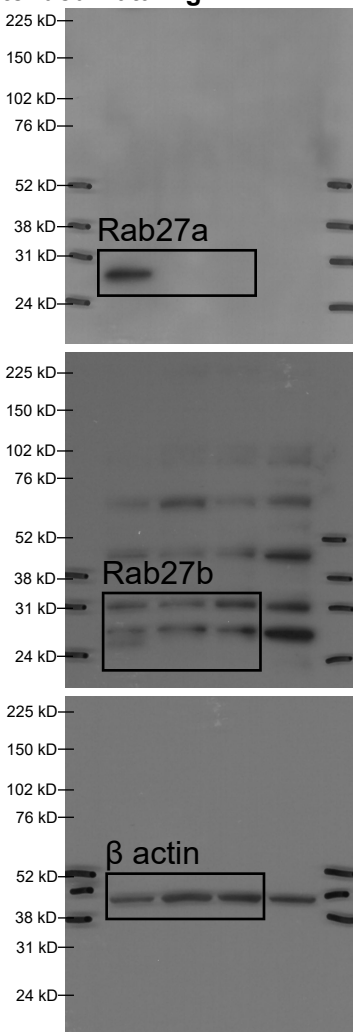

β actin, Rab27a and Rab27b were run on the same gel

Extended Data Fig. 3j

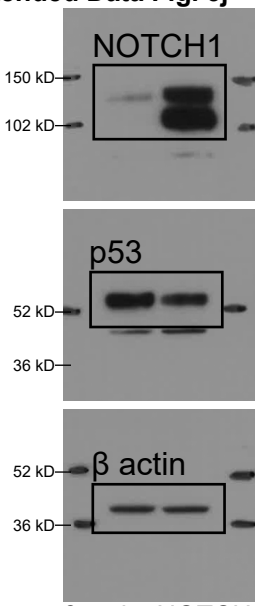

β actin, NOTCH1 and p53 were run on the same gel

Supplementary Table 1. Cardiovascular hemodynamics in mice treated with carvedilol

Measure	Carvedilol	Vehicle	*P*
Echocardiography			
Ejection fraction, %	68.19	65.80	0.502
Endocardial volume, diastole, µL	60.96	55.60	0.421
Endocardial volume, systole, µL	19.44	19.03	0.891
Arteriolar blood flow			
Diameter, µm	20.25	19.93	0.841
Blood flow rate, nL/min	506.28	487.02	0.470

N = 5 animals per group. Values indicate mean ; unpaired two-tailed t-test.

Supplementary Table 2. Patient characteristics

Characteristic		All patients			TH				
					Low (N = 33)		High (N= 37)		*P* value
Age, mean (range), years									0.204
		57.3	(22.1-84.1)		55.8	(22.1-84.1)	58.8	(22.3-83.8)	
Sex, N, %									0.457
Male		45	64%		23	70%	22	60%	
Female		25	36%		10	30%	15	40%	
T category, N, %									0.801
T1		10	14%		9	27%	1	3%	
T2		23	33%		7	21%	16	43%	
T3		13	19%		7	21%	6	16%	
T4a		24	34%		10	31%	14	38%	
N category, N, %									0.584
N0		17	24%		8	24%	9	24%	
N1		15	21%		9	27%	6	16%	
N2a-c		13	19%		6	18%	7	19%	
N3b		25	36%		10	31%	15	41%	
Treatment, N, %									0.578
Surgery		14	20%		8	24%	6	22%	
Surgery + RT		31	44%		15	46%	16	41%	
Surgery + CRT		25	36%		10	30%	15	27%	

Chi-square and Fisher's exact was used for sex, T classification, N classification and treatment categories; unpaired two-tailed t-test was used for age.

Supplementary Table 3. Multivariate analysis of survival

Measure	Overall survival			Recurrence-free survival		
	HR	95% CI	*P* value	HR	95% CI	*P* value
Unadjusted						
TH high	4.50	2.20-10.13	<0.0001	2.60	1.25-5.79	0.01
Adjusted						
TH high	15.64	3.55-93.11	0.0001	4.86	1.37-21.38	0.0135

Abbreviations: HR: hazard ratio, aHR: adjusted hazard ratio, CI: confidence interval, TH: tyrosine hydroxylase, ND: neural density. Adjusted to age, sex, AJCC 8 T classification, AJCC 8 N classification, treatment (surgery, surgery + radiation or surgery + chemoradiation), margin status (positive, ≤5 and >5 mm), and perineural invasion (present or absent). N=70 individual patients. Multivariate analyses were performed using Cox proportional hazard models.

Materials and Methods

Animals and in vivo *procedures*

Chemical sympathectomy (adrenergic denervation) was performed by intraperitoneal injection of 6-OHDA (Sigma-Aldrich), given at a first dose of 100 mg/kg (freshly dissolved in phosphate-buffered saline [PBS] before injection, to minimize oxidation), followed by a second and third dose of 250 mg/kg, 48 and 96 hours later. To evaluate the effect of the adrenergic antagonist and sympathectomy on blood flow, cardiac function was assessed by echocardiography using the Vevo 2100 ultrasound imaging system, in which mice were treated for 4 consecutive days with vehicle or carvedilol according to the protocol described above (n = 6 per group). For imaging, animals were anesthetized with a mixture of O_2/1.5% isoflurane and then positioned ventral side up on the platform of the imaging system. Echocardiography signal and respiratory rate were captured through the electrode pads on the advanced physiologic monitoring unit and transmitted to the Vevo system for monitoring. Cardiac examinations were performed in 2D images using the parasternal long axis view in B-mode with a 1MS550D 40-MHz probe. Two cineloops (300 frames per cineloop) were recorded per animal and then analyzed on four diastoles and four systoles per animal. The endocardial stroke volume and endocardial diastolic volume were determined to calculate the ejection fraction. To measure blood flow velocities, we used pulsed-wave Doppler mode and B-mode images. The single-beat mean diameter and velocity waveforms were time aligned and combined to achieve the diameter-velocity loop. Pulse-wave velocity (PWV) values were obtained from the slope of the linear part of the loop, which corresponds to the early systolic phase, using the formula PWV=0.5/slope [1,2].

For EV injection experiments BALB/c *nu/nu* mice were inoculated with 50,000 PCI-13–pBabe cells resuspended in 30 µL of serum-free Dulbecco modified Eagle medium (DMEM) into the tongue on day 0. On day 8, mice were randomly assigned to two groups (n = 12 each), and then EVs from either PCI-13–$p53^{WT}$ or PCI-13–pBabe ($p53^{Null}$) cells resuspended in 20 µL of PBS were

injected intratumorally once daily for 22 days. EVs injected into each tumor were harvested from the same number of cancer cells to the estimated number of cells comprising the tumor [3]. Briefly, fresh EVs were harvested for injection from supernatant 72 hours after plating of the cells; the total number of cells increased from 18 million to 144 million cells. EV dose was adjusted to cell number using the following formula: $Exosome\ amount\ (number\ of\ cells\ x\ days) = \int_0^3 18{,}000{,}000\, x2^x$. Tumor volume was monitored twice per week, and mice were killed on day 30 for harvesting of tongue tissue for further examinations.

Animals were randomly allocated to undergo surgical denervation or carvedilol/6-OHDA treatment before they underwent those interventions . For EV injection studies and orthotopic models with no intervention (other than tumor engraftment), animals were randomly allocated into experimental groups prior to cell inoculation. Investigators were blinded to group during the measurement of tumor size and mouse body weight except in the EV injection experiment.

Immunohistochemistry and histology

For preparation of tumor, tongue, and ganglia sections, tissues were fixed in 4% paraformaldehyde overnight at 4°C, then embedded in paraffin. For pathology analyses, paraffin-embedded tongue tissues were trimmed to full face, then sectioned at 5-μm thickness and stained with hematoxylin and eosin (H&E). For immunohistochemistry, tissue slices were incubated with primary antibodies overnight in blocking solution, followed by appropriate fluorophore-conjugated secondary antibodies, and counterstained with 4′,6-diamidino-2-phenylindole (DAPI). For non-fluorescent stains, sections were further processed for the ABC histochemical method (Vector).

Primary cultures immunofluorescence imaging. Matrigel-embedded DRG were fixated with 4% paraformaldehyde overnight at 4°C and blocked/permeabilized in PBS containing 10% horse serum and 1% Triton X-100 for 4 hours at room temperature. DRG were incubated with primary antibody in 5% horse serum with 0.01% Triton X-100 overnight at 4°C. Secondary antibody was

applied for 90 minutes at room temperature. Trigeminal ganglia neurons in primary culture (see *Cell Culture*): neurons for immunofluorescence staining were fixed with 4% paraformaldehyde for 10 minutes at room temperature. Cells were then gently washed three times with PBS and subsequently blocked in 5% horse serum and 0.025% Triton X-100 for 1 hour at room temperature. Primary staining was performed overnight at 4°C in the blocking buffer. Cells were again washed three times and then stained with secondary antibodies diluted in blocking buffer for 1 hour at room temperature.

Immunofluorescence images were acquired with a spinning disk confocal microscope (Andor Revolution WD, Yokogawa) attached to an inverted IX83 Olympus microscope equipped with a 60× 1.35 numerical aperture UPLSAPO objective lens. For quantification of neuritogenesis, images were analyzed using the FilamentTracer module in the Imaris software (Bitplane).

To quantify the proximity of adrenergic nerves and the vasculature in the oral cavity, images were analyzed using the Simple Neurite Tracer plugin [4] in the Fiji build of ImageJ (NIH) and TissueFinder in PerkinElmer inForm. We employed a combination of morphologic and proximity analysis. The overall surface area of each TH^+ nerve and TH^+ perivascular nerve was calculated and then weighted according to the vessel's surface area as a percentage of total nerve coverage in the image.

For *in vivo* analysis of cancer-associated neuritogenesis slides were imaged at 20× using the PerkinElmer Vectra platform and imported into the analytical module TissueFinder in PerkinElmer inform [5]. Then, the Vectra TIFF files were imported into the statistical programming language R, and the entire cross-sectional images of slides were manually analyzed in Pannoramic Viewer (3DHISTECH).

Cell sorting and flow cytometry

Primary sensory neurons were isolated from TG dissected from 6- to 8-week-old mice as previously described [6]. After ganglia dissection, tissue was enzymatically digested with papain (40 U/mL, EMD Millipore) for 20 minutes in 37°C followed by 20 minutes of digestion with collagenase II (4 mg/mL)/dispase II (4.6 mg/mL) solution. Using Percoll gradient, comprising 12.5% and 28% Percoll in complete L-15 medium (L-15 with 5% fetal calf serum, penicillin/streptomycin, HEPES), we separated the myelin and nerve debris from trigeminal neurons. All flow cytometric analyses were carried out using an LSR II flow cytometer running FACSDiva 8.0 software and FACSAria (all BD Biosciences). Data were analyzed by Kaluza (Beckman Coulter) software. To assess adrenergic differentiation and transdifferentiation by flow cytometry, cell suspensions were stained on ice with cell surface markers and transcription factors (see *Antibodies and staining reagents*).

Cell culture and in vitro *assays*

The OCSCC cell line PCI-13 lacking endogenous expression of p53 was obtained from the laboratory of Dr. Jennifer Grandis (University of Pittsburgh, Pittsburgh, PA) in August 2008 and engineered to stably express constructs containing wild-type p53 ($p53^{WT}$), null construct (pBabe, $p53^{Null}$), mutant p53 (R273H, C238F and G245D), as described previously [7]. The isogenic HNSCC cell lines HN30 (expressing $p53^{WT}$) and HN31 (expressing $p53^{Mut}$) were obtained in December 2008 from the laboratory of Dr. John Ensley (Wayne State University, Detroit, MI) and from Dr. Barbara Frederick (University of Colorado Health Sciences Center-Colorado), respectively. The cell lines were maintained in DMEM supplemented with 10% EV-depleted fetal bovine serum (Gibco, Thermo Fisher Scientific), L-glutamine, sodium pyruvate, nonessential amino acids, and vitamin solution and were incubated at 37°C in 5% CO_2 and 95% air. All human cell lines were authenticated upon arrival by STR profiling using 14 short tandem repeat (STR) loci including the gender determining locus, Amelogenin.

To assess neuritogenesis *in vitro*, primary sensory TG neurons were produced and plated on laminin-coated coverslips. Two hours after plating, 12 wells were flooded with 1 mL of warm (37°C) F-12 culture medium (Sigma-Aldrich) supplemented with 10% EV-depleted fetal bovine serum (Gibco, Thermo Fisher Scientific) and 1% penicillin/streptomycin and incubated at 37°C in 5% CO_2 and 95% air. For the *in vitro* paracrine co-culture of cancer cells with DRG, we harvested DRG from BALB/c *nu/nu* mice 2 to 4 weeks old as previously described [8]. The excised DRG were implanted at the bottom of the well in a growth factor–depleted Matrigel matrix (BD Biosciences). The carcinoma cells were plated on top of the transwell, and cultures were grown in Roswell Park Memorial Institute 1640 medium containing 10% EV-depleted fetal bovine serum in 37°C and 5% CO_2 incubation conditions (for primary cultures' immunofluorescence labeling and imaging, see *Immunohistochemistry and histology*).

Human DRG neurons were prepared as described previously [9]. Written informed consent for participation, including use of tissue samples, was obtained from each patient prior to inclusion. The protocol was reviewed and approved by The University of Texas MD Anderson Cancer Center Institutional Review Board, and all experiments conformed to relevant guidelines and regulations. Briefly, each donor was undergoing surgical treatment that necessitated ligation of spinal nerve roots to facilitate tumor resection or spinal reconstruction. Spinal roots were ligated proximal to the DRG, spinal roots were sharply cut both proximal and distal to the DRG, and excised DRG were transferred immediately into cold (~4°C) and sterile balanced salt solution containing nutrients. DRG were transported to the laboratory on ice in a sterile, sealed 50-mL centrifuge tube. Upon arrival to the laboratory, each ganglion was carefully dissected from the surrounding connective tissues and sectioned into several ~1- to- 2-mm pieces. DRG were digested in 2 mL of a mixed enzyme solution: 0.1% trypsin (Sigma-Aldrich, T9201), 0.1% collagenase Sigma-Aldrich, C1764; w/v, final concentration), and 0.01% DNase (Sigma-Aldrich, D5025) diluted in DMEM/F-12. The pieces of tissue were transferred to a 37°C rotator to shake

at a speed 124-128 revolutions/min. Every 20 minutes, tissue fragments were allowed to settle, and the supernatant/dissociated cells were collected and transferred to DMEM/F-12 with enzyme inhibitor. Supernatant was replaced with 2 mL of fresh digestion solution. The tissue was returned to the 37°C rotator, and this process was repeated until tissue fragments were well digested. Dissociated cells were centrifuged at 180 *rpm* for 5 minutes, supernatant was removed, and the cells were gently resuspended in culture medium with DMEM/F-12 supplemented with EV free 10% serum and 2 mM glutamine. Cells were plated onto laminin-coated µ-Slide 8 Well (ibidi) and cultured at 37°C with 5% CO_2 for 24-72 hours prior to undergoing transfection or labeling.

SYTO RNASelect–labeled miRNA transfer

Purified EVs derived from OCSCC cells were incubated at 37°C for 20 minutes in the presence of conditioned medium labeled with 500 nM SYTO RNASelect (s32703, Invitrogen). The medium was discarded, and the EVs were washed twice with EV spin columns (MW3000, Invitrogen) to remove excess dye. Labeled EVs were added to the dish in which neurons were seeded, and the cells were incubated at 37°C for 24 hours before imaging.

DiI-labeled EV transfer

Purified EVs derived from OCSCC cells were labeled with the CM-DiI tracer (C7000, Invitrogen). EVs were incubated with 2 µM CM-DiI for 5 minutes, washed twice with EV spin columns (MW3000, Invitrogen) to remove excess dye, and incubated with neurons at 37°C for 12 hours before imaging.

miRNA microarray expression analysis

For miRNA expression analysis, we used a customized single-channel Agilent array containing a collection of probes (sense and antisense) for various types of non-coding RNAs (human pre-miRNAs, mouse pre-miRNAs, ultra-conserved elements, pyknons, and long non-coding RNAs). Data pre-processing steps of background correction, normalization, and summarization were

performed in R version 3.4.1 using functions from the limma library. A threshold for positive spot selection for microarray data was calculated as the mean value of all the dark corner spots plus twice the standard deviation [10]. Linear models and empirical Bayes methods from limma were used to obtain the statistics and assess differential gene expression between two conditions. Statistical significance was defined as a *P* value of <0.05, and we imposed a cut-off of functional relevance on the fold change at an absolute value of 1.1. Cases with two probes associated with a gene displaying two opposite behaviors (one up and one down in the same comparison) were discharged from further analyses.

Catecholamine measurement

Tongues were freshly dissected and immediately homogenized in 0.1 M trichloroacetic acid containing 10^{-2} M sodium acetate, 10^{-4} M ethylenediaminetetraacetic acid, 5 ng/mL isoproterenol (as an internal standard), and 10.5% methanol (pH 3.8) and centrifuged at 10,000*g* for 20 minutes [11]. The supernatant was analyzed by enzyme-linked immunosorbent assay per the manufacturer's protocol to quantify noradrenaline (IBL America).

Transient miRNA transfection

mirVana miRNA mimics, miRNA inhibitors, and scramble controls were obtained from Ambion (inhibitors and miRNA mimics mir34a-5p: UGGCAGUGUCUUAGCUGGUUGU and miR141-5p: CAUCUUCCAGUACAGUGUUGGA). The AllStars Negative Control siRNA was purchased from QIAGEN. MISSION miRNA mimics and scramble controls were purchased from Sigma-Aldrich. miRNA mimics and miRNA inhibitors were transfected using the Lipofectamine RNAiMAX transfection reagent (Life Technologies) according to the manufacturer's protocol.

Analysis of TCGA data set of OCSCC patients

We considered the TCGA data set of OCSCC patients with available clinical information, pathology images, and mutation data. The data set comprised 231 patients including 104 events

of death with a median survival time of 595 days. For each patient, we morphologically quantified the neural tissue in the available H&E sections and then weighted as the number of neural filaments per field. Neural elements were identified by evaluation of all available H&E stained tumor sections for typical morphologic patterns of peripheral nerves (2-4 slides per patient, Extended data, Figure 1a) by a specialized Head and Neck pathologist.

Human tongue samples

Preexisting human formalin-fixed paraffin-embedded glossectomy samples were obtained for staining after approval by the MD Anderson internal review board. Informed consent for this study was obtained in accordance with The University of Texas MD Anderson institutional review board for human research. Patient characteristics including age, sex, and dates of surgery were adjusted for as shown in Supplementary Table 3. All patients underwent glossectomy and neck dissection and had histologically confirmed and clinically local or locoregional oral cavity cancer. For each patient, data on the primary tumor (tumor-node-metastasis classification system according to the American Joint Committee on Cancer [AJCC], 8th edition), perineural invasion, and surgical margin status were recorded, as well as adjuvant treatment administration (radiation therapy or concurrent chemoradiation). Recurrence was classified as local or distant at the time of data analysis; 31 recurrences were documented in this cohort of patients. The median follow-up among men without recurrence was 61 months. Depth of invasion and extranodal extension were analyzed using the AJCC 8th T and N classifications, respectively, and not as independent variables, to eliminate confounding [78]. Surgically resected primary tumors were paraffin embedded and serially sectioned (thickness 5 μm). For each block, a section was stained with H&E to localize normal areas among cancer. For each patient, 5 to 10 whole histologic consecutive sections were analyzed by two independent reviewers from MD Anderson to define the neural density. Nerve densities were assessed blind, without knowledge of histological diagnoses or clinical data. For each patient (n = 24), consecutive sections were stained for TH,

VAChT, and both neurofilament-light and neurofilament-heavy as described above to quantify adrenergic, cholinergic, and total autonomic nerve fiber densities, respectively, in tongue tumor areas and in remaining normal tongue tissues surrounding cancer areas. For each marker defined above, the mean of five representative fields (one field = 0.15 mm^2 for Olympus 20×/1.0 numerical aperture objective) was calculated from tumor and normal areas captured as described above.

For human survival predictor studies, we examined bivariate associations between each of the markers and the outcome variables. The association between TH expression and time to recurrence or death was determined using a Kaplan-Meier plot, and statistical significance was assessed by log-rank test (n = 70). To further estimate the magnitude of the association: a logistic regression model was used to estimate odds ratios and 95% confidence intervals for the associations between nerve densities in cancer tissue and times to tumor recurrence and death. Several steps of multivariate analysis were also conducted in the regression models with initial adjustments for age, sex, T and N classification, surgical margin status, and adjuvant treatment administration.

Immunoblotting

Immunoblotting was performed using lysates from whole-cell pellets samples in radioimmunoprecipitation assay buffer containing protease and phosphatase inhibitor cocktails (Sigma-Aldrich). Protein was quantified by Bradford assay (Bio-Rad), equal concentration of proteins (20 µg) were loaded on 4% to 20% acrylamide Criterion TGX precast gels (Bio-Rad) for Western blot analysis. Resolved proteins underwent semi-dry transfer to nitrocellulose membranes, which were then probed overnight with the following anti-human primary antibodies: Rab27A (Abcam, ab55667; mouse monoclonal, 1:500), Rab27B (Abcam, ab103418; rabbit polyclonal, 1:200), TP53 (DO-1) (Cell Signaling Technology, 18032; mouse monoclonal, 1:1,000), NOTCH1 (Cell Signaling Technology, rabbit, 1:1,000), HSP70 (Mouse Anti-Hsp70, BD Pharmingen, Cat. #: 554243, Lot #: 0000058171; 1:1000; 2 2 minutes exposure for EVs), and β-

actin (Sigma-Aldrich, A1978; mouse monoclonal, 1:5,000). Membranes were then incubated with appropriate horseradish peroxidase–conjugated secondary antibody, followed by incubation with SuperSignal West Femto substrate (Thermo Fisher Scientific), and chemoluminescent signal detected with autoradiographic paper.

Isolation of miRNAs

Total RNA was extracted from purified EVs using the total EV RNA isolation kit (Invitrogen) or from neurons using the QIAzol reagent and the miRNeasy Mini Kit (QIAGEN) according to the manufacturer's protocols. Patient miRNA (see *Human tongue samples)* was extracted from macroscopically dissected formalin-fixed paraffin-embedded specimens using the miRNeasy FFPE Kit (QIAGEN) according to the manufacturer's protocol.

Quantitative real-time polymerase chain reaction

Quantitative real-time PCR was performed as previously described [12]. miRNA expression was quantified using TaqMan miRNA assays (Applied Biosystems) and TaqMan probes for miRNAs and *RNU6* (Invitrogen and Sigma-Aldrich). PCR was performed in 96-well plates using the CFX96 Real-Time PCR System (Bio-Rad). All reactions were performed in triplicate. *RNU6* was used as an invariant control for assessing the expression of cellular miRNAs.

Establishment of stable cell lines

Stable OCSCC cell lines expressing miRNA inhibitor *hsa-miR-34a-5p* were generated by selection with puromycin (2 μg/mL). OCSCC cells at 90% confluency were transfected with Lenti microRNA Inhibitor expression vector (Sigma-Aldrich) in 24-well dishes using a multiplicity of infection value of 10 in accordance with the manufacturer's instructions. Cells were replated in a 10-cm dish 12 hours after transfection, followed by selection with puromycin for 3 weeks. Five surviving single colonies were picked from each transfectant and cultured for an additional 2 weeks. Quantitative real-time PCR was used to assess levels of target transcript, and the cells

expressing the highest amount of *miR-34a-5p* targets among the transfectants were considered to stably express miRNA inhibitor *hsa-miR-34a-5p* [13].

1 Di Lascio, N., Stea, F., Kusmic, C., Sicari, R. & Faita, F. Non-invasive assessment of pulse wave velocity in mice by means of ultrasound images. *Atherosclerosis* **237**, 31-37, doi:10.1016/j.atherosclerosis.2014.08.033 (2014).

2 Lee, L. *et al.* Aortic and Cardiac Structure and Function Using High-Resolution Echocardiography and Optical Coherence Tomography in a Mouse Model of Marfan Syndrome. *PLoS One* **11**, e0164778, doi:10.1371/journal.pone.0164778 (2016).

3 Countercurrents, S. & Narod, S. A. Disappearing breast cancers. *Curr Oncol* **19**, 59-60, doi:10.3747/co.19.1037 (2012).

4 Longair, M. H., Baker, D. A. & Armstrong, J. D. Simple Neurite Tracer: open source software for reconstruction, visualization and analysis of neuronal processes. *Bioinformatics* **27**, 2453-2454, doi:10.1093/bioinformatics/btr390 (2011).

5 Feng, Z. *et al.* Multispectral imaging of formalin-fixed tissue predicts ability to generate tumor-infiltrating lymphocytes from melanoma. *J Immunother Cancer* **3**, 47, doi:10.1186/s40425-015-0091-z (2015).

6 Malin, S. A., Davis, B. M. & Molliver, D. C. Production of dissociated sensory neuron cultures and considerations for their use in studying neuronal function and plasticity. *Nat Protoc* **2**, 152-160, doi:10.1038/nprot.2006.461 (2007).

7 Osman, A. A. *et al.* Evolutionary Action Score of TP53 Coding Variants Is Predictive of Platinum Response in Head and Neck Cancer Patients. *Cancer Res* **75**, 1205-1215, doi:10.1158/0008-5472.CAN-14-2729 (2015).

8 Na'ara, S., Gil, Z. & Amit, M. In Vitro Modeling of Cancerous Neural Invasion: The Dorsal Root Ganglion Model. *J Vis Exp*, e52990, doi:10.3791/52990 (2016).

9 Li, Y. *et al.* The Cancer Chemotherapeutic Paclitaxel Increases Human and Rodent Sensory Neuron Responses to TRPV1 by Activation of TLR4. *J Neurosci* **35**, 13487-13500, doi:10.1523/JNEUROSCI.1956-15.2015 (2015).

10 Vallee, M. *et al.* Identification of novel and known oocyte-specific genes using complementary DNA subtraction and microarray analysis in three different species. *Biol Reprod* **73**, 63-71, doi:10.1095/biolreprod.104.037069 (2005).

11 Zahalka, A. H. *et al.* Adrenergic nerves activate an angio-metabolic switch in prostate cancer. *Science* **358**, 321-326, doi:10.1126/science.aah5072 (2017).

12 Mitchell, P. S. *et al.* Circulating microRNAs as stable blood-based markers for cancer detection. *Proc Natl Acad Sci U S A* **105**, 10513-10518, doi:10.1073/pnas.0804549105 (2008).

13 Misso, G. *et al.* Mir-34: a new weapon against cancer? *Mol Ther Nucleic Acids* **3**, e194, doi:10.1038/mtna.2014.47 (2014).